A NOVEL MULTI-WAY POWER DIVIDER DESIGN WITH ARBITRARY COMPLEX TERMINATED IMPEDANCES

Jiuchao Li[1, *], Yuanan Liu[1], Shulan Li[1], Cuiping Yu[1], Yongle Wu[1, 2], and Ming Su[1]

[1]School of Electronic Engineering, Beijing University of Posts and Telecommunications, Beijing 100876, China

[2]State Key Laboratory of Millimeter Waves, Southeast University, Nanjing 210096, China

Abstract—A simple and analytical design methodology for a novel multi-way Bagley Polygon power divider with arbitrary complex terminated impedances is proposed in this paper. The design parameters including electrical lengths and characteristic impedances can be obtained by the provided closed-form mathematical expressions when complex terminated impedances are known. Moreover, for convenient test, we design an impedance transformer to transform the complex impedance into real impedance using an extension line, and especially a reflection coefficient chart to solve it. Four special cases of 3-way Bagley Polygon power divider operating at 2.4 GHz are fabricated and measured with different condition complex terminated impedances for the purpose of verification. Excellent agreement between simulation and measurement results proves the validity of the design method. The presented Bagley Polygon power divider exhibits 180° phase difference between any two adjacent output ports and 0° phase difference between two symmetrical output ports and is suitable for multi-antenna and differential antenna system. Furthermore, simple layouts lead to convenient design procedure and easy fabrication.

1. INTRODUCTION

The conventional Wilkinson power divider developed by Wilkinson [1] consists of two quarter-wavelength lines and operates in a single band. Many efforts have been made to enhance its performance, such as ultra-wideband and broadband power divider [2–5], tri-band or integrated with substrate integrated waveguide (SIW) and defected ground structure (DGS) technology power dividers [6, 7], compact coupled-line and stepped-impedance transmission lines dual-band Wilkinson power dividers [8, 9], and dual-band unequal Wilkinson power divider using asymmetric coupled-line [10]. More than that, Bagley Polygon power divider (BPPD) has no lumped elements, such as resistors, and can be easily extended to any number of output ports [11–19]. In order to overcome the large area at low frequency, reduced size 3-way and 5-way BPPDs, using two kinds of methods with open stubs, were presented in [11]. In [12, 13], a general design of compact multi-way divider similar to BPPD with simple design theory was introduced. In [14], a compact dual-frequency 3-way BPPD using composite right/left handed (CRLH) transmission lines with shunt connections of open and short stubs for comparison was implemented. Moreover, a loop-type compact 5-way BPPD for dual-band, wide-band operation and easy fabrication was presented in [15]. In [16], an optimum design of a modified 3-way Bagley rectangular power divider using least square was presented. Based on the generalized 3-way BPPD, dual-band pass band planar filter based on signal-interference techniques was presented in [17], and the described filter approach consists of transversal filtering sections made up of generalized Bagley-polygon four-port power divider. In [18], the planar multi-way BPPDs that can operate at two arbitrary frequencies using Π-type dual-band transformers were proposed. Multi-band miniaturized 3-way and 5-way BPPDs using non-uniform transmission line transformers were proposed in [19]. Obviously, typical power dividers are terminated with constant real-value resistances, while most microwave circuits require complex impedance transformers, especially in active circuits. Analytical methods for the transmission-line impedance transformer between two complex impedances are described [20, 21]. The allowed regions for the terminated complex impedances are given in [22].

In this paper, a novel multi-way BPPD with arbitrary complex terminated impedances is proposed. Different from the previous BPPD in [12], the terminated impedances in this paper are extended from real values (such as 50 Ohm) to arbitrary complex values. By using equivalent circuit analysis, simple and analytical design equations are obtained. In order to obtain the extended impedance line which is

used to transform complex termination impedance to 50 Ohm, Smith chart, especially reflection coefficient chart, is used. Once the complex terminated impedances are known, the characteristic impedances and electrical lengths can be determined. For verification, four cases of this BPPD are discussed, fabricated, and measured with different complex terminated impedances, and there is excellent agreement between simulated and measured results.

2. CIRCUIT STRUCTURE AND THE THEORY

2.1. Multi-way BPPD

Figure 1(a) depicts the proposed multi-way BPPD configuration. This is a $2n + 1$-way BPPD, and signals fed on port 1 are equally divided into $2n + 1$ parts. Here, $n = 1, 2, \ldots$. Without loss of generalization, the source at port 1 has internal impedance Z_S while the load at the
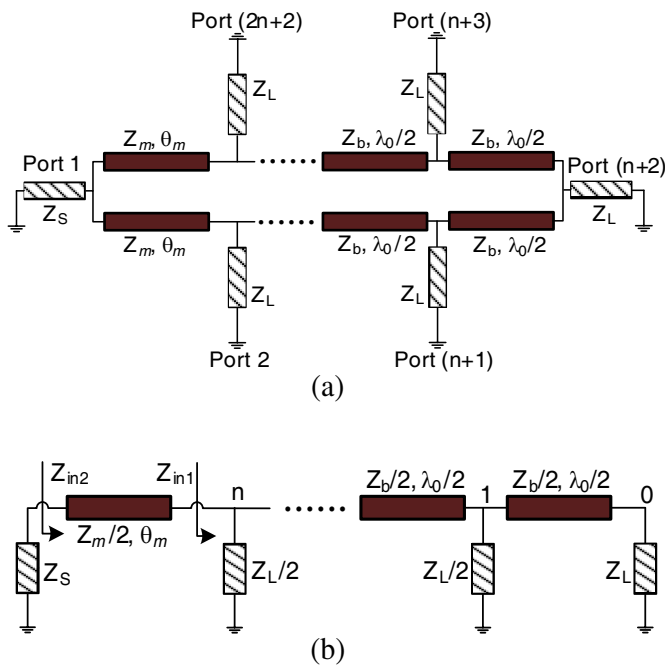

(a)

(b)

Figure 1. (a) Proposed multi-way BPPD configuration, and (b) equivalent circuit.

output ports has internal impedance Z_L. Here

$$Z_S = R_S + jX_S \tag{1}$$
$$Z_L = R_L + jX_L \tag{2}$$

The transmission line lengths between two adjacent output ports are decided to be $\lambda_0/2$, and those of the two lines separated from the input port to each two adjoining output ports are decided to be Z_m and θ_m. Because of symmetric configuration, the equivalent circuit of the $2n+1$-way BPPD can be equivalent to that in Figure 1(b). Here, Z_b and Z_m are the characteristic impedances of the $\lambda_0/2$ lines and θ_m lines, respectively. Z_{in1} is the input impedance looked from the right side of the θ_m line into the right side of it. By considering the input impedance formula, the input impedance Z_{in1} is then obtained as:

$$Z_{in1} = \frac{Z_L}{2n+1} \tag{3}$$

Considering the matching condition at the input port, we can obtain the value of Z_{in2} from Figure 1(b) as:

$$Z_{in2} = \left(\frac{Z_m}{2}\right) \frac{Z_{in1} + j\left(\frac{Z_m}{2}\right)\tan\theta_m}{\left(\frac{Z_m}{2}\right) + jZ_{in1}\tan\theta_m} \tag{4}$$

In order to match to Z_S, the following equation is necessary:

$$Z_{in2} = Z_S^* = R_S - jX_S \tag{5}$$

And (4) can be rewritten as:

$$R_S - jX_S = \left(\frac{Z_m}{2}\right) \cdot \frac{\left(\frac{R_L+jX_L}{2n+1}\right) + j\left(\frac{Z_m}{2}\right)\tan\theta_m}{\left(\frac{Z_m}{2}\right) + j\left(\frac{R_L+jX_L}{2n+1}\right)\tan\theta_m} \tag{6}$$

Rearranging (6) and separating the real and imaginary parts, we can obtain the following equations:

$$\begin{cases} \frac{Z_m}{2}\left(R_S - \frac{R_L}{2n+1}\right) + \frac{\tan\theta_m}{2n+1}(R_LX_S - X_LR_S) = 0 \\ \frac{Z_m}{2}\left(X_S + \frac{X_L}{2n+1} + \frac{Z_m\tan\theta_m}{2}\right) - \frac{\tan\theta_m}{2n+1}(R_LR_S + X_LX_S) = 0 \end{cases} \tag{7}$$

Solving (7), we found the closed-form solutions for Z_m and θ_m, and the results are:

$$Z_m = 2\sqrt{\left\{\frac{R_L(2n+1)\left(R_S^2 + X_S^2\right) - R_S\left(R_L^2 + X_L^2\right)}{(2n+1)\left[R_S(2n+1) - R_L\right]}\right\}} \tag{8}$$

$$\theta_m = \arctan\left\{\frac{Z_m\left[R_S(2n+1) - R_L\right]}{2\left(R_SX_L - R_LX_S\right)}\right\} \tag{9}$$

Here, the value of Z_b has no effect on matching of the proposed multi-way BPPD, and it is usual to make the value of Z_b equal to the value of Z_m. Thus, once the values of Z_S and Z_L are known, the value of Z_m, Z_b and θ_m can be determined by the closed-form Equations (8) and (9).

2.2. Impedance Transformer

Because of the Z_S or Z_L is a complex impedance, for the purpose of convenient test, we design an impedance transformer to transform the complex impedance Z_S or Z_L into real impedance Z_0, here, $Z_0 = 50\,\Omega$, using an extension line to solve the impedance transform between Z_S or Z_L and Z_0 [22]. An impedance transformer to transform complex impedance Z_A into real impedance Z_0 is depicted in Figure 2(a) where the characteristic impedance and electrical length of the impedance transformer are assumed to be Z_P and θ_P.
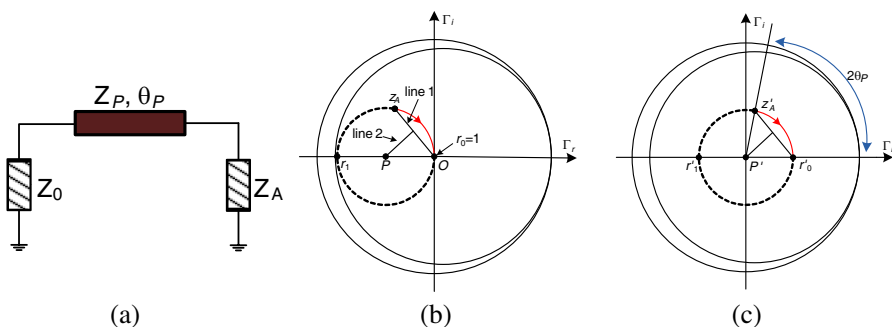

Figure 2. Impedance transformer of complex impedance into real impedance. (a) Impedance transformer with one transmission-line section, (b) two termination impedances are expressed on an impedance Smith chart normalized to Z_0, and (c) impedance Smith chart normalized to the characteristic impedance of Z_P.

The circle in Figure 2(b) intersects two points $r_0 = 1$ and r_1 on the real axis of reflection coefficients. The real and imaginary parts of the reflection coefficient are Γ_{rA} and Γ_{iA}, respectively. The normalized characteristic impedance $z_P = Z_P/Z_0$ of the impedance transformer is:

$$z_P = \sqrt{\frac{\Gamma_{rA} + \Gamma_{rA}^2 + \Gamma_{iA}^2}{\Gamma_{rA} - \left(\Gamma_{rA}^2 + \Gamma_{iA}^2\right)}} \tag{10}$$

The electrical length of the impedance transformer in Figure 2(a) is half the distance from z_A' to r_0' toward on the Smith chart as shown

Figure 2(c). Therefore, the electrical length θ_P may be found as:

$$\theta_P = 0.5 \cdot \left\{ \arctan\left(\frac{\Gamma_{iA'}}{\Gamma_{rA'}} \right) - \arctan\left(\frac{\Gamma_{i0'}}{\Gamma_{r0'}} \right) \right\} \tag{11}$$

where Γ'_{rA} and Γ'_{iA} are real and imaginary parts of reflection coefficient at z'_A, and Γ'_{r0} and $\Gamma'_{iA} = 0$ are those at r'_0.

Thus, if the information on z_A is given, the characteristic impedance of the impedance transformer and the electrical length in Figure 2(a) can be easily obtained using (10) and (11). It is necessary to point out that the reflection coefficients of z_A have a limit to obtain the impedance transformer and the electrical length. In order to match to Z_0 exactly, the following equations are necessary:

$$(\Gamma_{rA} - 0.5)^2 + \Gamma_{iA}^2 < 0.25, \qquad \Gamma_{rA} > 0 \tag{12a}$$

$$(\Gamma_{rA} + 0.5)^2 + \Gamma_{iA}^2 < 0.25, \qquad \Gamma_{rA} < 0 \tag{12b}$$

Therefore, the procedure to design the multi-way BPPD with arbitrary complex terminated impedances is briefly summarized as follows:

(1) According to the practical requirements, n is determined.

(2) According to Z_S and Z_L, the requisite characteristic impedances Z_m, Z_b, and electrical length θ_m are determined from (8) and (9).

(3) For the purpose of convenient test, the characteristic impedances Z_P, and electrical length θ_P of extension line are determined from (10) and (11).

3. SIMULATION AND EXPERIMENT

In order to verify the proposed design and analysis theory in Section 2, we take the 3-way BPPD as an example ($n = 1$). Based on the terminated impedances $Z_S = Z_0$ & $Z_L = Z_0$, $Z_S = Z_0$ & $Z_L = R_L + jX_L$, $Z_S = R_S + jX_S$ & $Z_L = Z_0$, and $Z_S = R_S + jX_S$ & $Z_L = R_L + jX_L$, four special cases of proposed 3-way BPPD operating at 2.4 GHz are designed, simulated, and fabricated. According to the different cases, simplify the design Equations (8) and (9), and determine requisite characteristic impedances Z_m, Z_b and electrical length θ_m. And then, determine the extension line from (10) and (11) to convenient test.

First, circuit models of the designed 3-way BPPDs are analyzed using Advanced Design System (ADS), and then, the proposed BPPDs are simulated using the electromagnetic (EM) simulator High Frequency Structure Simulator (HFSS). It is noted that the ideal lossless transmission lines are used in ADS simulation. A Rogers4350B substrate, with a dielectric constant of 3.48 and a thickness of 30 mil

is used. In the four special cases presented below, the terminating impedance Z_0 is chosen to be $50\,\Omega$. These special cases are summarized as follows (Case A to Case D).

3.1. Case A ($Z_S = Z_0$ & $Z_L = Z_0$)

When $Z_S = Z_0$ & $Z_L = Z_0$, this proposed 3-way BPPD becomes the conventional one as [12], and the design Equations (8) and (9) can be simplified as (13) and (14), respectively. The design parameters can be calculated, and details of the parameters are $Z_m = Z_b = 57.7\,\Omega$, $\theta_m = 90°$. According to these design parameters, the 3-way BPPD is designed, simulated, and fabricated. The amplitude and phase responses are shown in Figure 3. Figure 4 shows the photograph and physical dimensions of the fabricated 3-way BPPD,
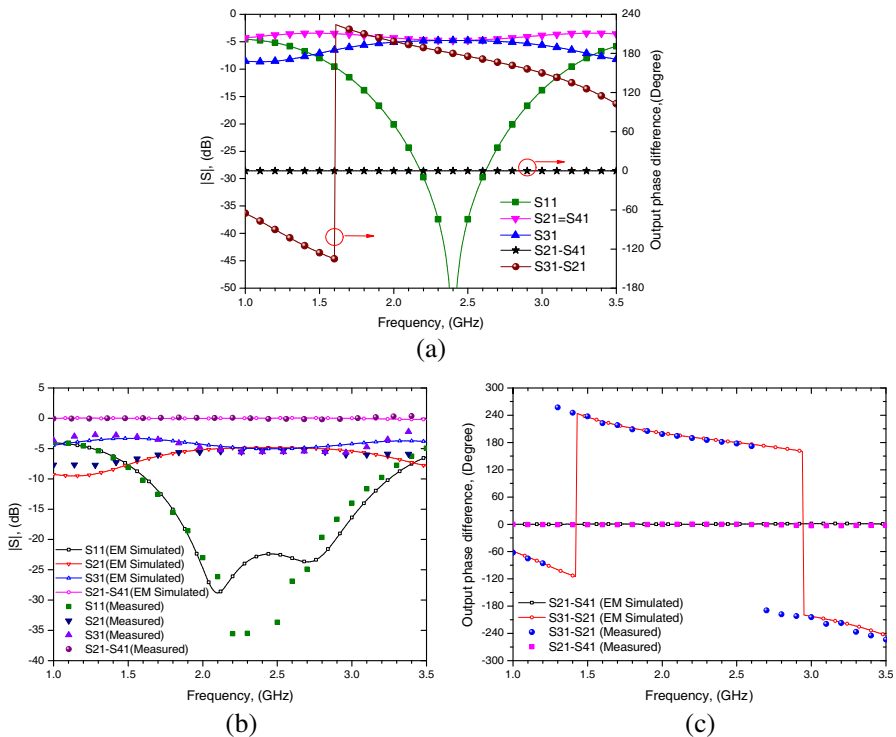

Figure 3. The amplitude and phase responses of the 3-way BPPD (Case A). (a) Simulated results of amplitude and phase responses with ADS. (b) Measured and EM simulated results of amplitude responses. (c) Measured and EM simulated results of phase responses.
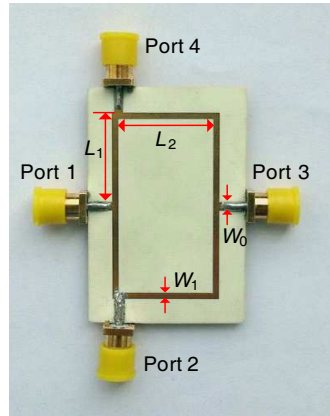
Figure 4. Photograph of the fabricated 3-way BPPD (Case A).

and the detailed dimensions are $L_1 = 720.75 \, \text{mil}$, $L_2 = 754 \, \text{mil}$, $W_1 = 52 \, \text{mil}$, and $W_0 = 66.5 \, \text{mil}$.

$$Z_m = Z_b = \frac{2Z_0}{\sqrt{2n+1}} = \frac{2Z_0}{\sqrt{3}} \tag{13}$$

$$\theta_m = 90^\circ \tag{14}$$

Figure 3(a) shows an excellent performance with the return loss of input port and insertion loss (4.77 dB). The BPPD has 180° phase difference between any two adjacent output ports and 0° phase difference between two symmetrical output ports. Figure 3(b) and Figure 3(c) show the measured and EM simulated results of amplitude and phase responses, respectively. The measured results are collected from Agilent N5230C network analyzer, and it can be seen that the EM simulated and measured results agree well. The amplitude of S_{11} is below −20 dB, from 1.92 to 2.82 GHz over a fractional bandwidth of about 38%, and the measured values of transmission parameters (S_{21}, S_{31}, and S_{41}) are approximately the same as EM simulated results, and the measured amplitude difference between two symmetrical output ports ±0.25 from 1.0 to 3.5 GHz. As shown in Figure 3(c), the measured phase difference between the two adjacent output ports is $180 \pm 5°$ from 2.29 to 2.57 GHz over a fractional bandwidth of about 11.5%, and the measured phase difference between two symmetrical output ports $0 \pm 1.6°$ from 1.0 to 3.5 GHz.

3.2. Case B ($Z_S = Z_0$ & $Z_L = R_L + jX_L$)

When $Z_S = Z_0$ & $Z_L = R_L + jX_L$, this proposed 3-way BPPD can be reduced to the input terminated impedance as real impedance Z_0, and the output terminated impedances are arbitrary complex impedances $Z_L = R_L + jX_L$. The design Equations (8) and (9) can be simplified as (15) and (16), respectively. Here, we assume the arbitrary complex impedance $Z_L = 55 + j10$. The design parameters can be calculated, and details of the parameters are $Z_m = Z_b = 60\,\Omega$, $\theta_m = 80°$. The extension line of Z_L transform into Z_0 can be determined from (10) and (11), denoted by the Z_{PL} and θ_{PL}. Solving Equations (10) and (11), the design parameters $Z_{PL} = 61\,\Omega$ and $\theta_{PL} = 32°$ are calculated. According to these design parameters, the 3-way BPPD is designed, simulated, and fabricated. The amplitude and phase
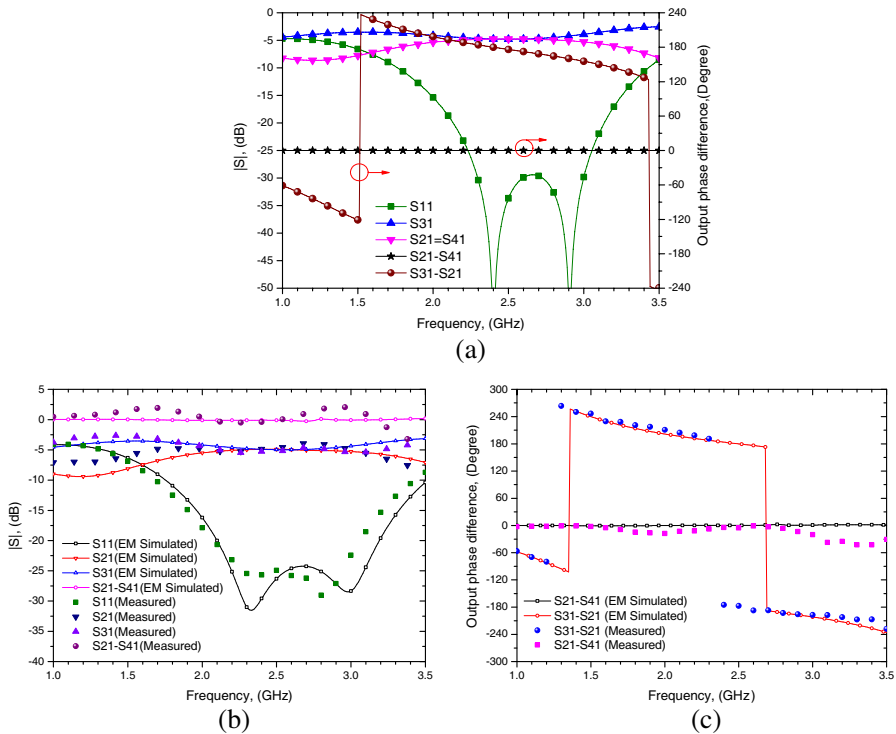

Figure 5. The amplitude and phase responses of the 3-way BPPD (Case B). (a) Simulated results of amplitude and phase responses with ADS. (b) Measured and EM simulated results of amplitude responses. (c) Measured and EM simulated results of phase responses.
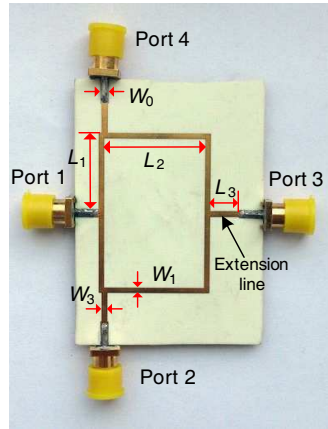
Figure 6. Photograph of the fabricated 3-way BPPD (Case B).

responses are shown in Figure 5. Figure 6 shows the photograph and physical dimensions of the fabricated 3-way BPPD, and the detailed dimensions are $L_1 = 639.05$ mil, $W_1 = 48.6$ mil, $L_2 = 840.3$ mil, $L_3 = 269.9$ mil, $W_3 = 47.2$ mil and $W_0 = 66.5$ mil.

$$
\begin{aligned}
Z_m = Z_b &= 2\sqrt{\left\{ \frac{R_L Z_0^2 (2n+1) - Z_0 \left(R_L^2 + X_L^2\right)}{(2n+1)\left[Z_0 (2n+1) - R_L\right]} \right\}} \\
&= 2\sqrt{\left\{ \frac{3R_L Z_0^2 - Z_0 \left(R_L^2 + X_L^2\right)}{3\left(3Z_0 - R_L\right)} \right\}}
\end{aligned} \tag{15}
$$

$$
\theta_m = \arctan\left\{ \frac{Z_m \left[Z_0 (2n+1) - R_L\right]}{2Z_0 X_L} \right\} = \arctan\left\{ \frac{Z_m \left(3Z_0 - R_L\right)}{2Z_0 X_L} \right\} \tag{16}
$$

From Figure 5, in Case B proposed 3-way BPPD shows an excellent performance with the return loss of input port and insertion loss. In particular, Figure 5(a) indicates ideal performance of BPPD with ADS simulated. Figure 5(b) and Figure 5(c) indicate the measured and EM simulated results of amplitude and phase responses, respectively. The input matching S_{11} is below -20 dB from 2.1 to 3.2 GHz, and the amplitude of S_{21}, S_{31} and S_{41} are approximately -4.8 dB at 2.4 GHz. But S_{21} has a little tolerance, and the BPPD has $4°$ phase difference between two adjacent output ports and $4°$ phase difference between two symmetrical output ports at 2.4 GHz. It is believed that the small discrepancies between the simulated and measured results were mainly caused by the fabrication tolerances.

3.3. Case C ($Z_S = R_S + jX_S$ & $Z_L = Z_0$)

When $Z_S = R_S + jX_S$ & $Z_L = Z_0$, this proposed 3-way BPPD can be reduced to the input terminated impedance as arbitrary complex impedances $Z_S = R_S + jX_S$, and the output terminated impedances are real impedance $Z_L = Z_0$. The design Equations (8) and (9) can be simplified as (17) and (18), respectively. Here, we assume the arbitrary complex impedance $Z_S = 30 - j5$. The design parameters can be calculated, and details of the parameters are $Z_m = Z_b = 46\,\Omega$, $\theta_m = 75°$. The extension line of Z_S transforming into Z_0 can be determined from (10) and (11), denoted by Z_{PS} and θ_{PS}. Solving Equations (10) and (11), the design parameters $Z_{PS} = 38\,\Omega$, $\theta_{PS} = 72°$ are calculated. According to these design parameters, the 3-way BPPD is designed, simulated, and fabricated. The amplitude and phase responses are shown in Figure 7. Figure 8 shows the photograph and physical
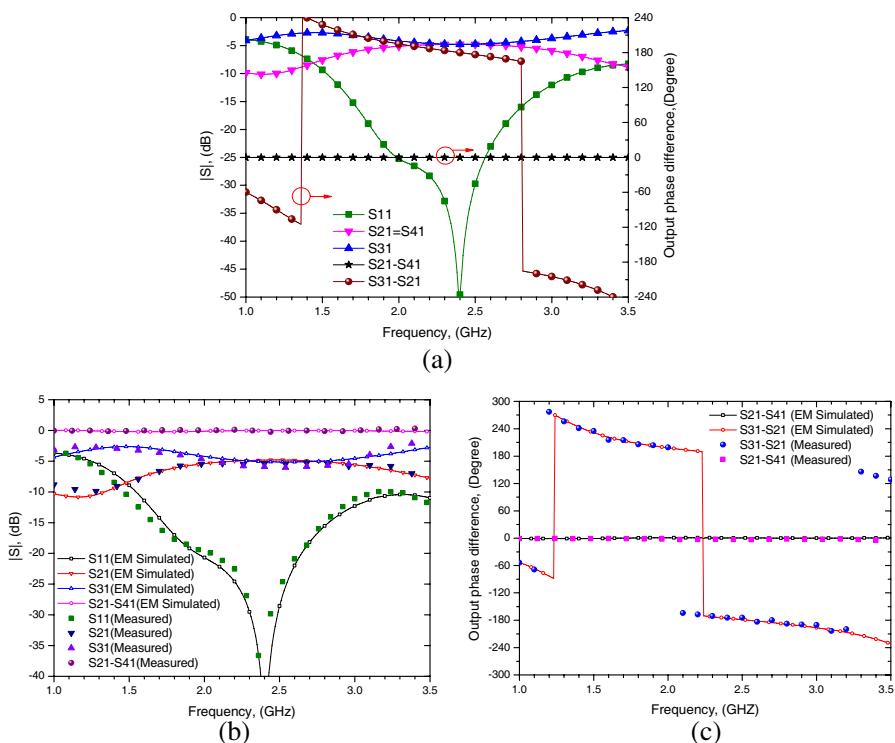

Figure 7. The amplitude and phase responses of the 3-way BPPD (Case C). (a) Simulated results of amplitude and phase responses with ADS. (b) Measured and EM simulated results of amplitude responses. (c) Measured and EM simulated results of phase responses.
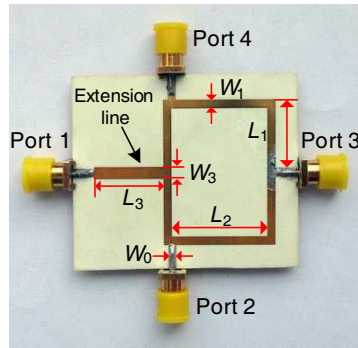
Figure 8. Photograph of the fabricated 3-way BPPD (Case C).

dimensions of the fabricated 3-way BPPD, and the detailed dimensions are $L_1 = 583.85$ mil, $W_1 = 75.7$ mil, $L_2 = 866.7$ mil, $L_3 = 632.15$ mil, $W_3 = 101.4$ mil and $W_0 = 66.5$ mil.

$$Z_m = Z_b = 2\sqrt{\left\{ \frac{Z_0 (2n+1)(R_S^2 + X_S^2) - R_S Z_0^2}{(2n+1)[R_S(2n+1) - Z_0]} \right\}}$$

$$= 2\sqrt{\left\{ \frac{3Z_0 (R_S^2 + X_S^2) - R_S Z_0^2}{3(3R_S - Z_0)} \right\}} \tag{17}$$

$$\theta_m = \arctan\left\{ \frac{Z_m [Z_0 - R_S(2n+1)]}{2Z_0 X_S} \right\} = \arctan\left\{ \frac{Z_m (Z_0 - 3R_S)}{2Z_0 X_S} \right\} \tag{18}$$

Figure 7(a) shows an excellent performance with the return loss of input port and insertion loss (4.77 dB). The BPPD has $180°$ phase difference between any two adjacent output ports and $0°$ phase difference between two symmetrical output ports at 2.4 GHz. Figure 7(b) and Figure 7(c) show the measured and EM simulated results of amplitude and phase responses, respectively. The measured results are collected from Agilent N5230C network analyzer, and it can be seen that the EM simulated and measured results agree well. The amplitude of S_{11} is below -20 dB from 2.03 to 2.64 GHz over a fractional bandwidth of about 26%, and the measured values of transmission parameters are approximately the same as EM simulated results, particularly, the measured amplitude difference between two symmetrical output ports ± 0.18 from 1.0 to 3.5 GHz. As shown in Figure 7(c), the measured phase difference between the two adjacent output ports is $180 \pm 5°$ from 2.36 to 2.74 GHz over a fractional bandwidth of about 15%, and the measured phase difference between two symmetrical output ports $0 \pm 2.8°$ from 1.0 to 3.5 GHz.

3.4. Case D ($Z_S = R_S + jX_S$ & $Z_L = R_L + jX_L$)

When $Z_S = R_S + jX_S$ & $Z_L = R_L + jX_L$, this proposed 3-way BPPD input terminated impedance is arbitrary complex impedances $Z_S = R_S + jX_S$, and the output terminated impedances are arbitrary complex impedances $Z_L = R_L + jX_L$. The design Equations (8) and (9) can be simplified as (19) and (20), respectively. Here, we assume $Z_S = 38 - j9$, $Z_L = 60 + j20$. The design parameters can be calculated, and details of the parameters are $Z_m = Z_b = 55\,\Omega$, $\theta_m = 49°$. The extension lines of Z_S and Z_L transforming into Z_0 can be determined from (10) and (11), denoted by Z_{PS}, θ_{PS} and Z_{PL}, θ_{PL}, respectively. Solving Equations (10) and (11), the design parameters $Z_{PS} = 39.5\,\Omega$, $\theta_{PS} = 47°$, $Z_{PL} = 70.5\,\Omega$ and $\theta_{PL} = 35.5°$ are calculated. According to these design parameters, the 3-way BPPD
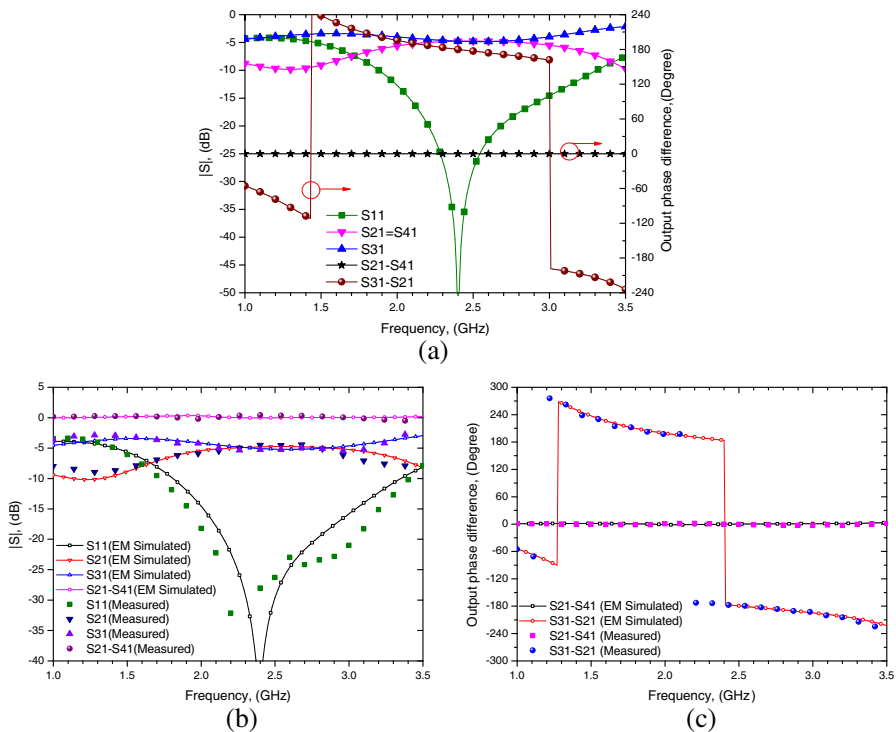

Figure 9. The amplitude and phase responses of the 3-way BPPD (Case D). (a) Simulated results of amplitude and phase responses with ADS. (b) Measured and EM simulated results of amplitude responses. (c) Measured and EM simulated results of phase responses.
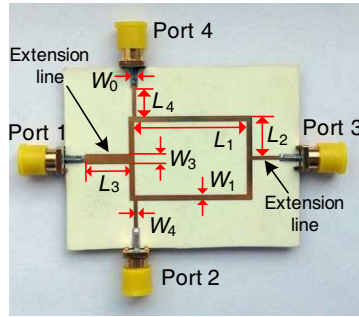
Figure 10. Photograph of the fabricated 3-way BPPD (Case D).

is designed, simulated, and fabricated. The amplitude and phase responses are shown in Figure 9. Figure 10 shows the photograph and physical dimensions of the fabricated 3-way BPPD, the detailed dimensions are $L_1 = 1095.4$ mil, $W_1 = 56.7$ mil, $L_2 = 389.55$ mil, $L_3 = 430$ mil, $W_3 = 95.8$ mil, $L_4 = 270$ mil, $W_4 = 35.7$ mil, and $W_0 = 66.5$ mil.

$$Z_m = Z_b = 2\sqrt{\left\{\frac{3R_L\left(R_S^2 + X_S^2\right) - R_S\left(R_L^2 + X_L^2\right)}{3\left(3R_S - R_L\right)}\right\}} \qquad (19)$$

$$\theta_m = \arctan\left\{\frac{Z_m\left(3R_S - R_L\right)}{2\left(R_S X_L - R_L X_S\right)}\right\} \qquad (20)$$

Figure 9(a) shows an excellent performance with the return loss of input port and transmission parameters (4.77 dB). The BPPD has 180° phase difference between any two adjacent output ports and 0° phase difference between two symmetrical output ports at 2.4 GHz. Figure 9(b) and Figure 9(c) show the measured and EM simulated results of amplitude and phase responses, respectively. The measured results are collected from Agilent N5230C network analyzer, and it can be seen that the EM simulated and measured results agree well. The amplitude of S_{11} is below -20 dB from 2.03 to 3.03 GHz over a fractional bandwidth of about 39.5%, and the measured values of transmission parameters are approximately the same as EM simulated results, particularly, the measured amplitude difference between two symmetrical output ports ± 0.25 from 1.0 to 3.5 GHz. As shown in Figure 9(c), the measured phase difference between the two adjacent output ports is $180 \pm 5°$ from 2.28 to 2.78 GHz over a fractional bandwidth of about 19.8%, and the measured phase difference between two symmetrical output ports $0 \pm 1.5°$ from 1.0 to 3.5 GHz.

In summary, there is excellent agreement between the measured results and the desired performances in these four cases. Judging from the preceding discussions, the performance of the four fabricated proposed 3-way BPPDs can fulfill our design goal and certify the validity of the proposed structures and the final closed-form design methods. Furthermore, the five or more ways BPPDs with arbitrary complex terminated impedances are suitable for implementation in this proposed concept.

4. CONCLUSION

In this paper, a novel multi-way BPPD with arbitrary complex terminated impedances is proposed, analyzed, designed, and implemented. The achieved design approach is analytical and simple. For convenient test, we design an impedance transformer to transform the complex impedance into real impedance using an extension line, especially reflection coefficient chart to solve it. Obviously, this proposed multi-way BPPD not only has simple plane structure, without reactive components, but also satisfies flexible input and output complex terminated impedances. For verification, four special cases of the 3-way BPPDs operating at 2.4 GHz are fabricated with different condition complex terminated impedances, and there is excellent agreement between the simulated and measured results. Moreover, this multi-way BPPD natural 180° phase difference between any two adjacent output ports and 0° phase difference between two symmetrical output ports make it suitable for multi-antenna, differential antenna system or other kinds of usages.

ACKNOWLEDGMENT

REFERENCES

1. Wilkinson, E., "An N-way hybrid power divider," *IRE Trans. Microw. Theory Tech.*, Vol. 8, No. 1, 116–118, 1960.

2. Chang, L., C. Liao, L. Chen, W. Lin, X. Zheng, and Y. Wu, "Design of an ultra-wideband power divider via the coarse-grained parallel micro-genetic algorithm," *Progress In Electromagnetics Research,* Vol. 124, 425–440, 2012.

3. Peng, H., Z. Yang, Y. Liu, T. Yang, and K. Tan, "An improved UWB non-coplanar power divider," *Progress In Electromagnetics Research,* Vol. 138, 31–39, 2013.

4. Lu, Y. L., G.-L. Dai, X. Wei, and E. Li, "A broadband out-of-phase power divider for high power applications using through ground via," *Progress In Electromagnetics Research,* Vol. 137, 653–667, 2013.

5. Wang, D., H. Zhang, T. Xu, H. Wang, and G. Zhang, "Design and optimization of equal split broadband microstrip Wilkinson power divider using enhanced particle swarm optimization algorithm," *Progress In Electromagnetics Research,* Vol. 118, 321–334, 2011.

6. Liu, W., F. Wei, and X.-W. Shi, "A compact tri-band power divider based on triple-mode resonator," *Progress In Electromagnetics Research,* Vol. 138, 283–291, 2013.

7. He, Z., J. Cai, Z. Shao, X. Li, and Y. Huang, "A novel power divider integrated with SIW and DGS technology," *Progress In Electromagnetics Research,* Vol. 139, 289–301, 2013.

8. Li, J., Y. Wu, Y. Liu, J. Shen, S. Li, and C. Yu, "A generalized coupled-line dual-band Wilkinson power divider with extended ports," *Progress In Electromagnetics Research,* Vol. 129, 197–214, 2012.

9. Deng, P., J. Guo, and W. Kuo, "New Wilkinson power dividers based on compact stepped-impedance transmission lines and shunt open stubs," *Progress In Electromagnetics Research,* Vol. 123, 407–426, 2012.

10. Dai, G. and M. Xia, "A dual-band unequal Wilkinson power divider using asymmetric coupled-line," *Journal of Electromagnetic Waves and Applications*, Vol. 25, Nos. 11–12, 1587–1595, 2011.

11. Wuren, T., K. Taniya, I. Sakagami, and M. Tahara, "Miniaturization of 3- and 5-way bagley polygon power dividers," *Asia-Pacific Microwave Conference (APMC) Proceedings*, Vol. 4, Dec. 2005.

12. Sakagami, I., T. Wuren, M. Fujii, and Y. Tomoda, "A new type of multi-way microwave power divider based on bagley polygon power divider," *Asia-Pacific Microwave Conference (APMC) Proceedings*, 1353–1356, 2006.

13. Sakagami, I., T. Wuren, M. Fujii, and M. Tahara, "Compact

multi-way power dividers similar to the Bagley polygon," *IEEE MTT-S Int. Microwave Symposium (IMS)*, 419–422, 2007.

14. Elles, D. and Y.-K. Yoon, "Compact dual band three way bagley polygon power divider using composite right/left handed (CRLH) transmission lines," *IEEE MTT-S Int. Microwave Symposium (IMS)*, 485–488, 2009.

15. Sakagami, I. and T. Wuren, "Compact multi-way power dividers for dual-band, wide-band and easy fabrication," *IEEE MTT-S Int. Microwave Symposium (IMS)*, 489–492, 2009.

16. Oraizi, H. and S. A. Ayati, "Optimum design of a modified 3-way Bagley rectangular power divider," *Mediterranean Microwave Symposium (MMS)*, 25–28, 2010.

17. Gomez-Garcia, R. and M. Sanchez-Renedo, "Application of generalized bagley-polygon four-port power dividers to designing microwave dual-band bandpass planar filters," *IEEE MTT-S Int. Microwave Symposium (IMS)*, 580–583, 2010.

18. Liu, X., C. Yu, Y. Liu, S. Li, F. Wu, and Y. Wu, "Design of planar dual-band multi-way power dividers," *Asia-Pacific Microwave Conference (APMC) Proceedings*, 722–725, 2010.

19. Shamaileh, K., A. Qaroot, and N. Dib, "Non-uniform transmission line transformers and their application in the design of compact multi-band Bagley power dividers with harmonics suppression," *Progress In Electromagnetics Research*, Vol. 113, 269–284, 2011.

20. Milligan, T. A., "Transmission-line transformation between arbitrary impedances," *IEEE Trans. Microw. Theory Tech.*, Vol. 24, No. 3, 159, 1976.

21. Potok, M. H. N., "Comments on 'Transmission-line transformation between arbitrary impedances'," *IEEE Trans. Microw. Theory Tech.*, Vol. 25, No. 1, 77, 1977.

22. Ahn, H. R., "Complex impedance transformers consisting of only transmission-line sections," *IEEE Trans. Microw. Theory Tech.*, Vol. 60, No. 7, 2073–2084, 2012.